Engineering 5 (2019) 243–249

Contents lists available at ScienceDirect

Engineering

journal homepage: www.elsevier.com/locate/eng

Research
High Performance Structures: Building Structures and Materials—Article

Steel Design by Advanced Analysis: Material Modeling and Strain Limits

Leroy Gardner *, Xiang Yun, Andreas Fieber, Lorenzo Macorini

Department of Civil and Environmental Engineering, Imperial College London, London SW7 2AZ, UK

ARTICLE INFO

Article history:
Received 31 July 2018
Revised 10 September 2018
Accepted 12 November 2018
Available online 26 February 2019

Keywords:
Advanced analysis
Continuous strength method
Local buckling
Material modeling
Strain limits

ABSTRACT

Structural analysis of steel frames is typically performed using beam elements. Since these elements are unable to explicitly capture the local buckling behavior of steel cross-sections, traditional steel design specifications use the concept of cross-section classification to determine the extent to which the strength and deformation capacity of a cross-section are affected by local buckling. The use of plastic design methods are restricted to Class 1 cross-sections, which possess sufficient rotation capacity for plastic hinges to develop and a collapse mechanism to form. Local buckling prevents the development of plastic hinges with such rotation capacity for cross-sections of higher classes and, unless computationally demanding shell elements are used, elastic analysis is required. However, this article demonstrates that local buckling can be mimicked effectively in beam elements by incorporating the continuous strength method (CSM) strain limits into the analysis. Furthermore, by performing an advanced analysis that accounts for both geometric and material nonlinearities, no additional design checks are required. The positive influence of the strain hardening observed in stocky cross-sections can also be harnessed, provided a suitably accurate stress–strain relationship is adopted; a quad-linear material model for hot-rolled steels is described for this purpose. The CSM strain limits allow cross-sections of all slenderness to be analyzed in a consistent advanced analysis framework and to benefit from the appropriate level of load redistribution. The proposed approach is applied herein to individual members, continuous beams, and frames, and is shown to bring significant benefits in terms of accuracy and consistency over current steel design specifications.

© 2019 THE AUTHORS. Published by Elsevier LTD on behalf of Chinese Academy of Engineering and Higher Education Press Limited Company. This is an open access article under the CC BY-NC-ND license (http://creativecommons.org/licenses/by-nc-nd/4.0/).

1. Introduction

The most recent editions of many international structural design codes permit the use of geometrically and materially nonlinear analysis, also known as advanced analysis, for the design of steel structures consisting of compact cross-sections. Examples include Section 5 of EN 1993-1-1 [1], Appendix D of AS 4100 [2], and Appendix 1 of AISC 360 [3]. The analysis is typically performed using the finite element (FE) method, and structural members are commonly represented using beam elements. The benefits of advanced analysis design are widely recognized [4–10]. Compared with the traditional approach to structural design, whereby the structural analysis is followed by individual member and cross-section checks, in advanced analysis, global frame and member instabilities (i.e., P-Δ and P-δ) are captured and the need for subsequent member checks is eliminated. However, since beam elements cannot capture local buckling, plastic analysis methods are currently limited to stocky cross-sections that possess sufficient rotational capacity for plastic hinges to develop and a collapse mechanism to form.

To avoid using complex shell elements for a global frame analysis, structural design codes generally account for local buckling by providing limitations on cross-section capacity and deformability by introducing discrete cross-section classes based on plate width-to-thickness ratios. However, this approach creates artificial "steps" in the capacity predictions of structural frames. For example, a Class 1 cross-section is assumed to have infinite rotation capacity, while a Class 2 cross-section is assumed to have zero.

In this paper, a more consistent design approach is proposed, whereby strain limits are used to mimic local buckling in an advanced structural analysis using beam elements. The strain limits are based on the continuous strength method (CSM) [11,12] and control the degree of plastic redistribution that occurs within the structure, taking due account of the local slenderness of the constituent cross-sections. Hence, structures with cross-sections of

* Corresponding author.
E-mail address: Leroy.gardner@imperial.ac.uk (L. Gardner).

https://doi.org/10.1016/j.eng.2018.11.026
2095-8099/© 2019 THE AUTHORS. Published by Elsevier LTD on behalf of Chinese Academy of Engineering and Higher Education Press Limited Company.
This is an open access article under the CC BY-NC-ND license (http://creativecommons.org/licenses/by-nc-nd/4.0/).

any class can be treated using beam elements in the same consistent manner. To capture the stress–strain characteristics of structural carbon steels accurately, a quad-linear material model has been developed [13] and incorporated into the CSM framework for the design of hot-rolled steel cross-sections under different loading conditions [14,15]; this material model is employed herein. In the proposed approach to design by advanced analysis, the structural resistance is taken as the lower of either ① the peak load factor reached during the analysis or ② the load factor at which the CSM strain limit is first reached. Note that, as recommended in Ref. [16], connections will generally have to be checked separately.

This paper outlines the framework required to include strain limits in design by advanced analysis. The quad-linear material model for hot-rolled steel is described and worked examples illustrate the benefits and general applicability of the proposed method. It should be noted that the following discussion is limited to the in-plane behavior of individual members, continuous beams, and frames consisting of hot-rolled steel I-shaped sections under major axis bending.

2. Material modeling

A typical engineering stress–strain curve for hot-rolled structural carbon steel subjected to quasi-static tensile load is shown in Fig. 1. In the elastic range, the slope is linear and is defined by the modulus of elasticity, or Young's modulus E, which is taken as 210 000 $N \cdot mm^{-2}$ according to EN 1993-1-1. After reaching the yield stress f_y, with the corresponding strain of $\varepsilon_y = f_y/E$, the strain continues to increase along a yield plateau without any apparent increase in stress. When the strain reaches the strain-hardening strain, ε_{sh}, strain hardening initiates and the stress begins to increase again with increasing strain. Finally, the stress reaches a maximum value at the ultimate tensile strength f_u and the corresponding ultimate strain ε_u. Beyond this point, necking and eventually fracture occur.

The stress–strain relationship for structural carbon steels is often idealized by an elastic-perfectly plastic model, and this simplified model generally forms the basis of the current design provisions in EN 1993-1-1. However, this model fails to capture the strain-hardening characteristics of the material, which are important for advanced computational and design methods such as the CSM, particularly for stocky cross-sections. Thus, a quad-linear

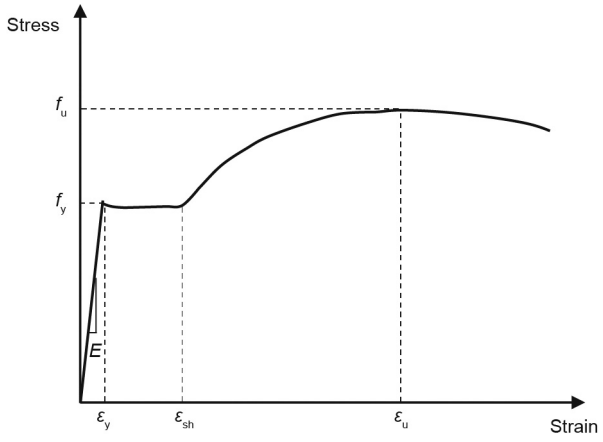

Fig. 1. A typical engineering stress–strain curve for hot-rolled structural carbon steel. E: Young's modulus; f_y: yield stress; ε_y: strain corresponds to f_y; f_u: ultimate tensile strength; ε_u: ultimate strain corresponds to f_u; ε_{sh}: strain-hardening strain.

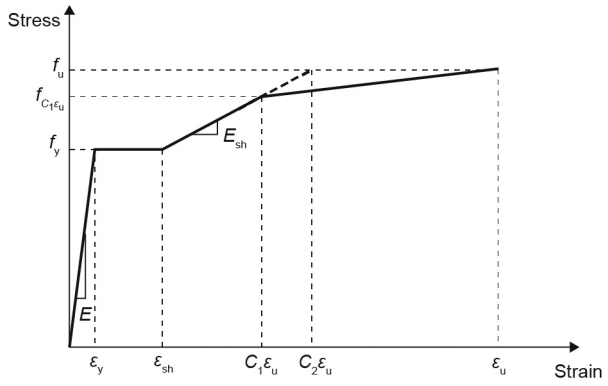

Fig. 2. Quad-linear material model for hot-rolled structural carbon steel.

material model, as illustrated in Fig. 2 and described by Eq. (1) [13], has been proposed to represent accurately the yield plateau and strain-hardening behavior of hot-rolled structural carbon steels, based upon and calibrated against a large dataset of tensile coupon test results. Two material coefficients (C_1 and C_2) are used in Eq. (1): C_1 defines a "cut-off" strain to avoid over-predictions of material strength and is also included in the CSM base curve, as described in Section 3.2; and C_2 is employed in Eq. (2) to determine the strain-hardening slope E_{sh}. These two coefficients may be determined respectively from Eqs. (3) and (4), which are expressed in terms of the strain-hardening strain ε_{sh} and the ultimate strain ε_u.

$$f(\varepsilon) = \begin{cases} E\varepsilon & \text{for } \varepsilon \le \varepsilon_y \\ f_y & \text{for } \varepsilon_y < \varepsilon \le \varepsilon_{sh} \\ f_y + E_{sh}(\varepsilon - \varepsilon_{sh}) & \text{for } \varepsilon_{sh} < \varepsilon \le C_1\varepsilon_u \\ f_{C_1\varepsilon_u} + \dfrac{f_u - f_{C_1\varepsilon_u}}{\varepsilon_u - C_1\varepsilon_u}(\varepsilon - C_1\varepsilon_u) & \text{for } C_1\varepsilon_u < \varepsilon \le \varepsilon_u \end{cases} \quad (1)$$

$$E_{sh} = \frac{f_u - f_y}{C_2\varepsilon_u - \varepsilon_{sh}} \quad (2)$$

$$C_1 = \frac{\varepsilon_{sh} + 0.25(\varepsilon_u - \varepsilon_{sh})}{\varepsilon_u} \quad (3)$$

$$C_2 = \frac{\varepsilon_{sh} + 0.4(\varepsilon_u - \varepsilon_{sh})}{\varepsilon_u} \quad (4)$$

The values of ε_{sh} and ε_u may be predicted from Eqs. (5) and (6), respectively. As a result, only three basic parameters are required for the quad-linear material model: E, f_y, and f_u. This model has recently been incorporated into the CSM for the design of hot-rolled steel cross-sections [14,15], and shows improved accuracy over the EN 1993-1-1 design provisions.

$$\varepsilon_{sh} = 0.1\frac{f_y}{f_u} - 0.055 \quad \text{but } 0.015 \le \varepsilon_{sh} \le 0.03 \quad (5)$$

$$\varepsilon_u = 0.6\left(1 - \frac{f_y}{f_u}\right) \quad \text{but } \varepsilon_u \ge 0.06 \quad (6)$$

Typical comparisons between measured stress–strain curves [17–19] and those generated using the developed quad-linear material model (Eq. (1)) and the predictive expressions of Eqs. (2)–(6) are shown in Figs. 3–5, revealing consistently accurate agreement for different steel grades. Further comparisons are presented and discussed by Yun and Gardner [13].

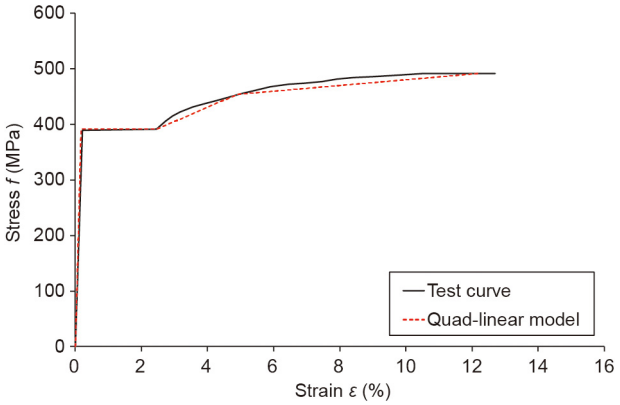

Fig. 3. Comparison of the quad-linear material model with an experimental stress–strain curve for grade S235 steel, as tested by Yun et al. [17].

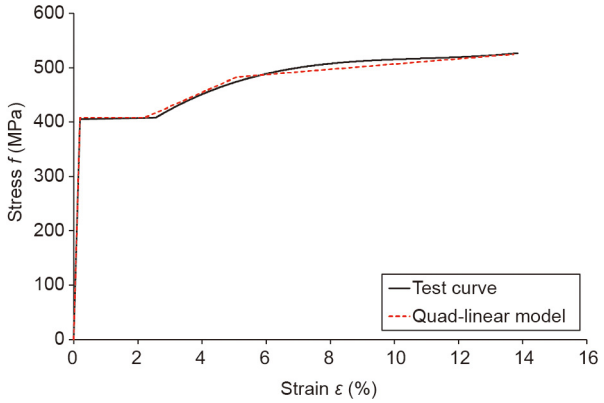

Fig. 4. Comparison of the quad-linear material model with an experimental stress–strain curve for grade S355 steel, as tested by Chan and Gardner [18].

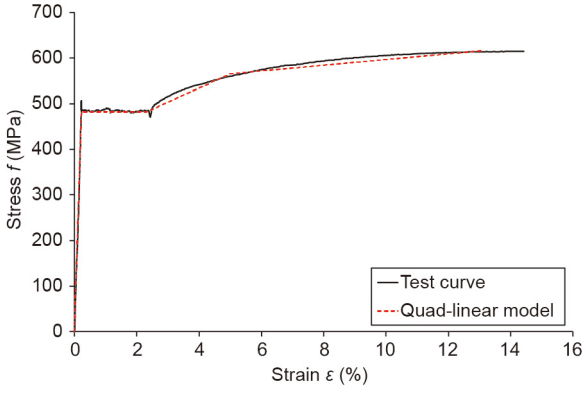

Fig. 5. Comparison of the quad-linear material model with an experimental stress–strain curve for grade S460 steel, as tested by Wang et al. [19].

3. Design by advanced analysis

3.1. Introduction

To account for the complex behavior of steel structures, both geometric and material nonlinearities should generally be considered. Traditionally, any limit state that is not included in the structural analysis must be accounted for using appropriate design checks. For example, a linear (first-order) analysis does not capture member buckling; thus, a corresponding member buckling check is required. Advanced analysis reduced the number of required design checks by incorporating various limit states into the analysis itself.

Ideally, all design checks can be eliminated and the capacity of a structural system defined simply by the peak load factor reached during the analysis. However, although frame and member instability (i.e., P-Δ and P-δ) effects are generally accounted for in an advanced analysis, more complex phenomena such as local buckling (and other cross-section level buckling modes) cannot be captured using beam elements and are thus typically excluded from the analysis and considered approximately through cross-section classification and corresponding capacity checks. The design approach proposed herein departs from this practice and employs the CSM strain limits to mimic the effects of local buckling in beam elements. It is hence possible to use the same advanced nonlinear analysis with beam elements for structures comprising cross-sections of all four classes, since the strain limits control the degree of local buckling, spread of plasticity, and plastic redistribution in a rational manner. This is in contrast to the step-wise treatment in current design codes, whereby full global plastic redistribution is allowed in the case of Class 1 cross-sections, while no redistribution is permitted for other classes of cross-section.

3.2. Continuous strength method and strain limits

The CSM is a deformation-based design approach that relates the cross-section slenderness to the deformation capacity [11]. Instead of classifying cross-sections into discrete groups, the CSM base curve defines the peak strain that a cross-section can endure. Utilizing this strain limit, integration of the corresponding stress distribution obtained from the adopted material model (see Section 2) over the area of the cross-section yields the cross-section capacity. Including the CSM strain limits in advanced analysis enables the CSM cross-section capacity to be computed directly, since numerical integration is performed at each load increment of the analysis.

The CSM base curve, shown in Fig. 6, provides a continuous relationship between the cross-section slenderness $\bar{\lambda}_p$ and its deformation capacity. The latter is defined in normalized form as $\varepsilon_{csm}/\varepsilon_y$, where ε_{csm} is the maximum compressive strain a cross-section can sustain and ε_y is the yield strain. The base curve is split into two parts: Eq. (7) applies to non-slender sections with $\bar{\lambda}_p \leq 0.68$, which are referred to as Class 1 to 3 cross-sections in EN 1993-1-1, and Eq. (8) applies to slender cross-sections with $\bar{\lambda}_p > 0.68$, which are referred to as Class 4 cross-sections in EN 1993-1-1. Note that in Eq. (7), two upper bounds have been placed on the predicted CSM strain ratio $\varepsilon_{csm}/\varepsilon_y$; the first limit Ω defines the level of plastic

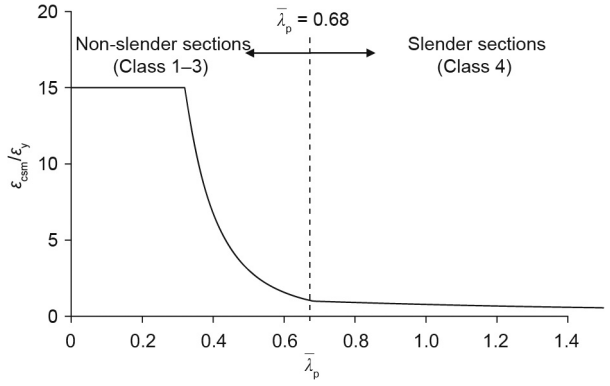

Fig. 6. CSM base curve: a continuous relationship between cross-section slenderness $\bar{\lambda}_p$ and its deformation capacity $\varepsilon_{csm}/\varepsilon_y$.

deformation that is deemed tolerable at ultimate limit state on a given project with a recommended value of 15, while the second limit of $C_1\varepsilon_u$, where C_1 is a material coefficient described in Section 2 and ε_u is the material ultimate strain which may be determined using Eq. (6), defines a "cut-off" strain to avoid over-predictions of material strength. Also note that both Eqs. (7) and (8) pass through the identified transition point, that is, (0.68, 1) in Fig. 6, thus ensuring compatibility between the CSM base curves for non-slender and slender cross-sections.

$$\frac{\varepsilon_{csm}}{\varepsilon_y} = \frac{0.25}{\bar{\lambda}_p^{3.6}} \quad \text{but} \quad \frac{\varepsilon_{csm}}{\varepsilon_y} \leq \min\left(\Omega, \frac{C_1\varepsilon_u}{\varepsilon_y}\right) \quad \text{for } \bar{\lambda}_p \leq 0.68 \tag{7}$$

$$\frac{\varepsilon_{csm}}{\varepsilon_y} = \left(1 - \frac{0.222}{\bar{\lambda}_p^{1.05}}\right)\frac{1}{\bar{\lambda}_p^{1.05}} \quad \text{for } \bar{\lambda}_p > 0.68 \tag{8}$$

The accuracy of the CSM strain limits used in advanced analysis depends on the ability to accurately determine the cross-section slenderness. The cross-section slenderness is a dimensionless parameter that quantifies susceptibility to local instability and is defined by Eq. (9), where f_y is the yield stress and σ_{cr} is the elastic critical buckling stress.

$$\bar{\lambda}_p = \sqrt{\frac{f_y}{\sigma_{cr}}} \tag{9}$$

Various methods are available to calculate the elastic critical buckling stress. Standard plate theory, utilizing buckling coefficients k such as those presented in EN 1993-1-5 [20], is simple to use yet ignores any element interaction by assuming simply supported boundary conditions along the adjoined plate edges. The elastic critical buckling stress can then be calculated using Eq. (10), where t and b are the relevant plate thickness and width, v is the Poisson's ratio; the plate element with the lowest buckling stress is then used to define the cross-section slenderness through Eq. (9).

$$\sigma_{cr} = k\frac{\pi^2 E}{12(1-v^2)}\left(\frac{t}{b}\right)^2 \tag{10}$$

Alternatively, approximate expressions calibrated against numerical results [21,22] may be used to determine the elastic critical buckling stress of the full cross-section. Plate interaction is implicitly accounted for in these expressions, which increases their accuracy. The expressions in Ref. [21] only cover pure compression and pure major/minor axis bending, whereas in structural frames, cross-sections are typically subjected to a combination of compression and bending; the expressions developed in Ref. [22] address this limitation and cover compression, bending and combined compression plus bending. Numerical tools, such as the constrained and unconstrained finite strip method (CUFSM) [23], can also be used to determine the elastic critical buckling stress of the full cross-section; CUFSM is employed in the present study.

3.3. Strain-averaging approach

Experiments [24,25] have shown that the maximum in-plane bending resistance of a member is greater under a moment gradient than under uniform bending. The increase in capacity arises from the restraint afforded to the critical section (i.e., that is under maximum bending moment) by the lower stressed adjacent regions, thus delaying the onset of local buckling in both the elastic and plastic regimes. A moment gradient is of course present in most practical applications, yet EN 1993-1-1 and the CSM base curve do not consider the effects of local moment gradients on the local stability of cross-sections.

It is proposed to exploit the beneficial influence of moment gradients on local stability by applying the CSM strain limit to a strain extracted from the advanced analysis that is averaged over a finite member length, as opposed to considering simply the most highly stressed (or strained) cross-section, as is customary. Since local buckling requires a finite length of member over which to develop—that is, the local buckling half-wavelength L_b—this represents a suitable distance over which to average the strains. This approach is in line with the observations of Lay and Galambos [26], who demonstrated experimentally that inelastic local buckling commences only when yielding has extended to a finite length of member related to the local buckling half-wavelength. By applying the CSM strain limit to an averaged strain, it is therefore possible to directly account for the magnitude of the local moment gradient; under uniform moment, the averaging approach predicts the cross-section capacity, while for increasing moment gradients, the peak moment capacity increases accordingly. The strain-averaging approach also reduces the sensitivity of the strength predictions to the mesh density employed in the FE model.

4. Implementation

4.1. General

In this section, the proposed advanced analysis is applied to a series of individual members, as well as continuous beams and a frame, in order to illustrate how the CSM strain limits are able to mimic local buckling, control the level of inelastic redistribution of forces and moments, and capture the beneficial effects of moment gradients. For comparison, the capacity predictions according to EN 1993-1-1 are also shown. In all cases, calibrated shell FE models featuring local geometric imperfections were employed to provide benchmark results. The shell models were developed in Abaqus [27] and solved using the modified Riks method [28]. The quad-linear material model described in Section 2 was adopted in the simulations.

4.2. Beams

The normalized bending capacity at the critical cross-section of a series of beams with cross-sections of different local slenderness analyzed under four-point bending and as a cantilever is shown in Fig. 7, where M_{max} is the maximum bending moment, M_{pl} is the plastic moment capacity, and M_{el} is the elastic moment capacity. It may be seen that application of the CSM strain limits to the beam element models yields safe-sided predictions of the shell FE model results across the range of cross-section slenderness. According to EN 1993-1-1, there is an artificial "step" in bending capacity from Class 2 to 3 cross-sections, which can be eliminated using the modified elastic–plastic bending capacity [29] to account for partial yielding in Class 3 cross-sections. For Class 4 cross-sections, the strain limits predict similar capacities to Eurocode 3 but avoid the cumbersome calculation procedures associated with the effective width method. The shell FE models capture an increase in bending capacity of 5%–10% across the range of cross-section slenderness from the uniform moment case to the cantilever case, due to the beneficial influence of the moment gradient. Similarly, the proposed advanced analysis using beam elements accurately predicts an increase of 2%–7% due to the moment gradient, which is accounted for through the strain-averaging approach. On the other hand, EN 1993-1-1 does not capture this effect and does not distinguish between the two cases, but predicts a single bending capacity for each cross-section.

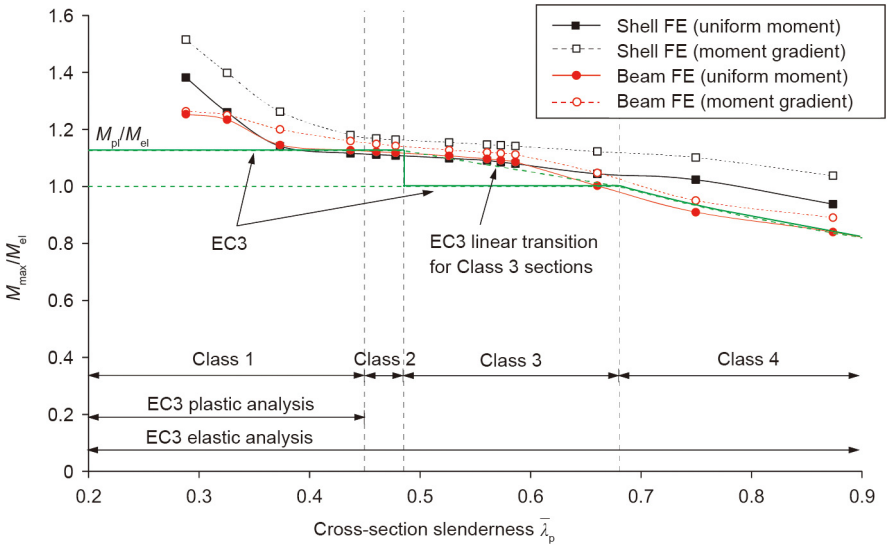

Fig. 7. Normalized bending capacity predictions from the shell FE model, proposed approach (i.e., beam FE model with strain limits), and EN 1993-1-1 for beams under uniform moment and a moment gradient with varying cross-section slenderness. EC3: EN 1993-1-1.

4.3. Continuous beams

At an isolated member level, there is no scope to allow for moment redistribution. In indeterminate structures, however, such as continuous beams, the benefits of the proposed method can become even more significant. In addition to the local cross-section strength and the effects of moment gradients, the collapse load of an indeterminate system depends on the level of inelastic force and moment redistribution. Fig. 8 shows the ultimate load factor at collapse, α_u, normalized by the load factor at which the first yield occurs, α_{el}, for shell FE models of a series of continuous beams under point loads P multiplied by load factor α, along with the capacity predictions from the proposed method of design by advanced analysis and Eurocode 3. EN 1993-1-1 only permits the use of plastic analysis methods, which are able to capture the redistribution of forces and moments as the material yields, for Class 1 cross-sections. On the other hand, Class 2 cross-sections must be analyzed elastically and thus benefit from no redistribution, even though some yielding occurs before their plastic moment capacity is reached. The resulting steps in resistance predictions clearly do not reflect the shell FE results and are an overly simplistic representation of reality. The use of a consistent advanced analysis, in which the CSM strain limits define the cross-section dependent level of permissible redistribution, is shown to provide significantly more accurate capacity prediction. The average capacity prediction for the 46 analyzed continuous beams according to EN 1993-1-1 is 0.810 of the shell FE results, with a coefficient of variation (COV) of 5.3%. In comparison, the proposed method of design by advanced analysis predicts a mean capacity of 0.924 of the shell FE results, with a COV of 4.9%.

4.4. Frames

Considering structural behavior at the frame level, a slightly modified version of "Test frame 2," as reported by Avery and Mahendran [30], is used to illustrate the full benefits of the proposed design method. The single bay portal frame comprised a single Class 3 cross-section throughout. Compared with the original

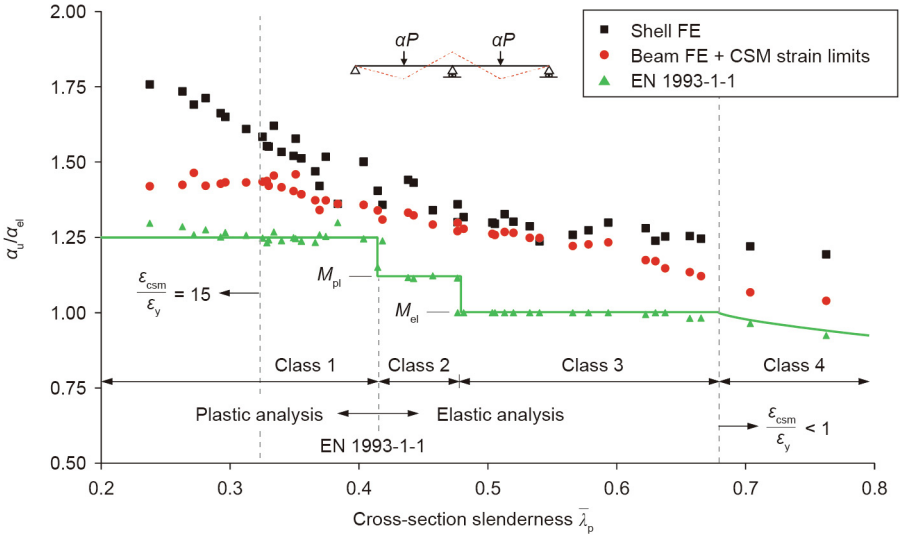

Fig. 8. Normalized bending capacity predictions from the shell FE model, proposed approach (i.e., beam FE model with strain limits), and EN 1993-1-1 for two-span continuous beams with mid-span point loads and varying cross-section slenderness.

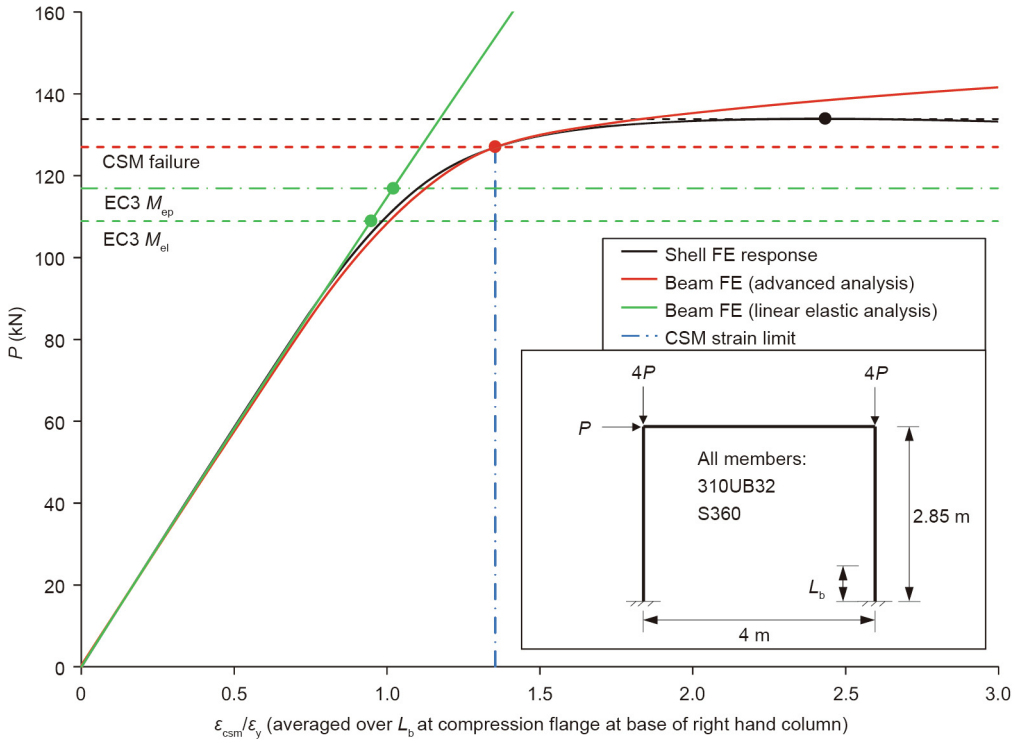

Fig. 9. Normalized load–strain response for a frame with a Class 3 cross-section. *P*: load of the frame; M_{ep}: the elastic-plastic moment.

test frame, the material model was adjusted to the quad-linear material model described earlier with an elastic modulus $E = 200\,000$ MPa, a yield stress $f_y = 360$ MPa, and an ultimate stress $f_u = 510$ MPa, matching the measured flange material properties of "Test frame 2." The global sway imperfection was based on the recommendations of EN 1993-1-1, while the member imperfections were taken as $l/1000$ in the most unfavorable direction, where l is the member length; both *P*-Δ and *P*-δ effects are therefore directly accounted for in the advanced analysis.

The load versus normalized strain (averaged over L_b from the critical cross-section) responses of the shell and beam FE models of the single bay portal frame are shown in Fig. 9. The measured test collapse load of the frame was $P = 135.0$ kN. In the shell FE model, some yielding is observed at the base of the right column prior to local buckling and ultimately collapse of the frame at a load of $P = 133.9$ kN. In contrast, the beam FE model cannot capture the local buckling at the base of the column and reaches a global sway failure at a peak load of $P = 156.0$ kN when allowing for unlimited strains—clearly an unsafe situation, since the shell FE collapse load is over-predicted by 16%.

To ensure safe capacity predictions, suitable cross-section and member design checks are required by EN 1993-1-1 following an elastic analysis of the structure; failure is predicted at a load of $P = 108.9$ kN. This is conservative by 20% compared with the shell FE model, since no account or benefit is taken from the spread of plasticity. Allowing for partial plastification in Class 3 cross-sections using a linear transition from the plastic to the elastic bending moment capacity through the elastic-plastic moment M_{ep} [29] increases the failure load prediction to $P = 116.9$ kN.

The proposed method of design by advanced analysis defines failure of the frame as the load level at which the CSM strain limit of $1.35\varepsilon_y$ for a modeled cross-section with $\bar{\lambda}_p = 0.626$ is reached (which occurs first at the base of the right-hand column). This occurs at a load level of $P = 127.0$ kN, which is only 6% shy of the shell FE collapse load. It should be emphasized again that the strains considered in the averaging procedure are the extreme fiber compressive flange strains of all elements fully contained within L_b. The described frame example illustrates both the ease of application of the proposed approach and the enhancements in design efficiency that can be achieved.

5. Conclusions

Beam finite elements are commonly used to analyze steel structures. Plastic analysis methods are limited to compact cross-sections that possess sufficient rotational capacity for plastic hinges to develop and rotate to form a plastic collapse mechanism. A new method of design by advanced analysis is presented, whereby local buckling is mimicked by applying cross-section-dependent strain limits obtained from the CSM. The proposed method is able to capture the beneficial effects of local moment gradients and predict realistic levels of force and moment redistribution. It is shown that the proposed method is more accurate than the current Eurocode 3 design approach, and thus represents a step forward in enhancing the sophistication and efficiency of structural steel design through advanced analysis.

Compliance with ethics guidelines

Leroy Gardner, Xiang Yun, Andreas Fieber, and Lorenzo Macorini declare that they have no conflict of interest or financial conflicts to disclose.

References

[1] EN 1993-1-1: Eurocode 3—design of steel structures—Part 1-1: general rules and rules for buildings. European standard. Brussels: European Committee for Standardization; 2005.
[2] AS 4100: Steel structures. Australian standard. Sydney: Standards Australia; 1998.
[3] AISC 360-16: Specification for structural steel buildings. American national standard. Chicago: American Institute of Steel Construction; 2016.
[4] Liew JYR, Chen WF, Chen H. Advanced inelastic analysis of frame structures. J Construct Steel Res 2000;55(1–3):245–65.

[5] Chen WF. Advanced analysis for structural steel building design. Front Archit Civ Eng China 2008;2(3):189–96.
[6] Kim SE, Chen WF. Design guide for steel frames using advanced analysis program. Eng Struct 1999;21(4):352–64.
[7] Trahair NS, Chan SL. Out-of-plane advanced analysis of steel structures. Eng Struct 2003;25(13):1627–37.
[8] Buonopane SG, Schafer BW. Reliability of steel frames designed with advanced analysis. J Struct Eng 2006;132(2):267–76.
[9] Rasmussen KJR, Zhang H, Cardoso F, Liu W. The direct design method for cold–formed steel structural frames. In: Proceedings of the 8th International Conference on Steel and Aluminium Structures; 2016 Dec 7–9; Hong Kong, China.
[10] Surovek AE. Advanced analysis in steel frame design: guidelines for direct second-order inelastic analysis. Reston: American Society of Civil Engineers; 2012.
[11] Gardner L. The continuous strength method. Proc Inst Civ Eng Struct Build 2008;161(3):127–33.
[12] Gardner L, Yun X, Macorini L, Kucukler M. Hot-rolled steel and steel-concrete composite design incorporating strain hardening. Structures 2017;9: 21–8.
[13] Yun X, Gardner L. Stress-strain curves for hot-rolled steels. J Construct Steel Res 2017;133:36–46.
[14] Yun X, Gardner L, Boissonnade N. The continuous strength method for the design of hot-rolled steel cross-sections. Eng Struct 2018;157:179–91.
[15] Yun X, Gardner L, Boissonnade N. Ultimate capacity of I-sections under combined loading—Part 2: parametric studies and CSM design. J Construct Steel Res 2018;148:265–74.
[16] Zhang H, Shayan S, Rasmussen KJR, Ellingwood BR. System-based design of planar steel frames, I: reliability framework. J Construct Steel Res 2016;123:135–43.
[17] Yun X, Gardner L, Boissonnade N. Ultimate capacity of I-sections under combined loading—Part 1: experiments and FE model validation. J Construct Steel Res 2018;147:408–21.
[18] Chan TM, Gardner L. Bending strength of hot-rolled elliptical hollow sections. J Construct Steel Res 2008;64(9):971–86.
[19] Wang J, Afshan S, Gkantou M, Theofanous M, Baniotopoulos C, Gardner L. Flexural behaviour of hot-finished high strength steel square and rectangular hollow sections. J Construct Steel Res 2016;121:97–109.
[20] EN 1993-1-5: Eurocode 3—design of steel structures—Part 1–5: plated structural elements. European standard. Brussels: European Committee for Standardization; 2006.
[21] Seif M, Schafer BW. Local buckling of structural steel shapes. J Construct Steel Res 2010;66(10):1232–47.
[22] Gardner L, Fieber A, Macorini L. Formulae for calculating elastic local buckling stresses of full structural cross-sections. Structures 2019;17:2–20.
[23] Li Z, Schafer BW. Buckling analysis of cold-formed steel members with general boundary conditions using CUFSM: conventional and constrained finite strip methods. In: Proceedings of the 20th International Speciality Conference on Cold-Formed Steel Structures; 2010 Nov 3–4; Saint Louis, MO, USA. Rolla: Missouri University of Science and Technology; 2010. p. 17−31.
[24] Lay MG. The experimental bases of plastic design—a survey of the literature. Fritz laboratory report. Bethlehem: Fritz Engineering Laboratory, Department of Civil Engineering, Lehigh University; 1964 Sep. Report No.: 297.3. Publication No.: 258.
[25] Gioncu V, Petcu D. Available rotation capacity of wide-flange beams and beam-columns. Part 2. Experimental and numerical tests. J Construct Steel Res 1997;43(1–3):219–44.
[26] Lay MG, Galambos TV. The inelastic behavior of beams under moment gradient. Fritz Engineering Laboratory Report. Bethlehem: Lehigh University; 1964. Report No.: 197.
[27] Dassault Systemes Simulia Corp. Abaqus analysis user's manual, version 6.13. Providence: Dassault Systemes; 2013.
[28] Crisfield MA. A fast incremental/iterative solution procedure that handles 'snap-through'. Comput Struct 1981;13(1–3):55–62.
[29] Greiner R, Lechner A, Kettler M. Background information to design guidelines for cross-section and member design according to Eurocode 3 with particular focus on semi-compact sections. Graz: Institute for Steel Structures and Shell Structures; 2012.
[30] Avery P, Mahendran M. Large-scale testing of steel frame structures comprising non-compact sections. Eng Struct 2000;22(8):920–36.